

1 **Hall Effect on Tearing Mode Instabilities in Tokamak**

2 W. Zhang, Z. W. Ma and S. Wang

3 Institute for Fusion Theory and Simulation, Department of Physics, Zhejiang University,
4 Hangzhou 310027, China

5 **Abstract.** Tearing mode instability is one of the most important dynamic processes in space and
6 laboratory plasmas. Hall effects, resulted from the decoupling of electron and ion motions, could
7 cause the fast development and perturbation structure rotation of the tearing mode and become
8 non-negligible. A high accuracy nonlinear MHD code (CLT) is developed to study Hall effects on
9 the dynamic evolution of tearing modes with Tokamak geometries. It is found that the
10 diamagnetic rotation of the mode structure is self-consistently contained in the Hall MHD model.
11 The self-consistently generated rotation largely alters the dynamic behaviors of the double tearing
12 mode.

13 I. INTRODUCTION

14 It is widely believed that many eruptive phenomena in both space^{1, 2} and laboratory^{3, 4} are
15 closely related to a tearing mode instability⁵ that leads to not only magnetic energy converting into
16 kinetic energy and heat^{6, 7} but also the barrier breaking down between two different plasma
17 regions. It is regarded as the primary cause for the degradation of plasma performance in magnetic
18 confined fusion device such as Tokamak⁸⁻¹⁰. The tearing mode instability was firstly studied
19 analytically by Furth et al¹¹ in the framework of resistive magnetohydrodynamics (MHD). It is
20 found that the linear growth rate of the resistive tearing mode instability is $\gamma \sim S^{-3/5}$, where S is
21 Lundquist number.

22 The Hall-MHD model which describes two-fluid plasma with massless electron is often used
23 to study magnetic reconnection¹²⁻¹⁴. It is believed that Hall effects can largely accelerate dynamic
24 process of magnetic reconnection. The reconnection rate in Hall MHD well agrees with that in full
25 particle simulation. Most studies of magnetic reconnection are carried out in slab geometry where
26 there is no diamagnetic drift effect which may play an important role in dynamics of tearing mode
27 instability in a toroidal geometry such as magnetic confined fusion device Tokamak.

28 Effects of diamagnetic drift on linear tearing mode instability were firstly studied by Ara et
29 al¹⁵ in the framework of the two-fluid MHD. In previous simulations of the m/n=1/1 resistive kink
30 instability and sawtooth, a diamagnetic drift is included as an initial velocity.^{16, 17} In the present
31 study, we carry out a Hall-MHD simulation with the zero initial velocity. It is found that the
32 tearing mode structure is rotated diamagnetically.

33 One of an advanced mode in Tokamak is operated with a reversed shear q profile,^{18, 19} where q
34 is the safety factor. The system may be subject to the double tearing mode (DTM) instability
35 which is excited in neighboring rational surfaces. DTM could have quite different dynamic
36 process from a single tearing mode due to mutual interaction between two tearing mode
37 instabilities in rational surfaces. The tearing mode instabilities in two rational surfaces could
38 excite each other if their perturbations in two rational surfaces are anti-phase, i.e., the expansion of
39 the island in one rational surface compresses the current sheet of another rational surface. The
40 tearing mode instabilities in two rational surfaces could be suppressed each other if their
41 perturbations in two rational surfaces are in-phase, i.e., the expansion of the island in one rational

42 surface collides with the expansion of the island in another rational surface. Since the tearing
 43 mode structures in Hall MHD are rotated due to diamagnetic drift, it is worthwhile to investigate
 44 dynamic process of the double tearing mode instability when the pressure gradients are different in
 45 the two rational surfaces.

46 To the best of our knowledge, a toroidal tokamak simulation in the framework of Hall-MHD
 47 has not been carried out. In this paper, Hall MHD simulations are performed to investigate the
 48 dynamic processes of the $m/n=2/1$ tearing mode and the $m/n=3/1$ double tearing mode by the CLT
 49 code^{20,21} developed at Zhejiang University.

50 Our article is organized as follows. In Section II, without the initial diamagnetic drift velocity,
 51 the diamagnetic rotation frequency associated with the tearing mode instability in the linear stage
 52 is derived based on Hall MHD. In Section III, the Hall MHD equations used in CLT are presented.
 53 In Section IV.A, we present simulation results from toroidal Hall-MHD code (CLT) and compare
 54 these results with theoretical predictions. In Section IV.B, double tearing mode instability is
 55 simulated with the different pressure gradients in two rational surfaces. Finally, we summarize our
 56 work in Section VI.

57

58 **II. DIAMAGNETIC RTOTATION FOR TEARING MODE INSTABILITY DUE TO HALL** 59 **EFFECTS**

60 The diamagnetic rotation frequency is firstly derived by Ara et al¹⁵. They used two-fluid
 61 equations and analyzed the effects of diamagnetic rotation on the tearing mode instability. In this
 62 section, we use the incompressible Hall MHD equations to derive the diamagnetic rotation
 63 frequency and we will show that the theoretical prediction is in good agreement with our
 64 simulation results in Section IV.A.

65 For the sake of the simplicity, incompressible assumption $\nabla \cdot \mathbf{u} = 0$ is used. In cylindrical
 66 geometry, the linearized equations for tearing mode instability⁵ can be written as

$$67 \quad \gamma \psi_{h1} - \psi'_{h0} \gamma \xi = \frac{\eta}{\mu_0} \left[\frac{1}{r} \frac{d}{dr} \left(r \frac{d\psi_{h1}}{dr} \right) - \left(\frac{m^2}{r^2} + \frac{n^2}{R^2} \right) \psi_{h1} \right] \quad (1)$$

$$\begin{aligned}
& \gamma^2 \rho \frac{1}{m} \left[\frac{1}{r} \frac{d}{dr} \left(r \frac{d(r\xi)}{dr} \right) - \frac{m^2}{r^2} (r\xi) \right] \\
68 \quad & = -\frac{m}{\mu_0 r} \psi'_{h0} \left[\frac{1}{r} \frac{d}{dr} \left(r \frac{d\psi_{h1}}{dr} \right) - \frac{m^2}{r^2} \psi_{h1} \right] + \frac{m}{r} \psi_{h1} \frac{dJ_{z0}}{dr}
\end{aligned} \tag{2}$$

69 where ψ_{h0} and ψ_{h1} are initial helical flux and perturbed helical flux, respectively. ξ is a
70 radical displacement. In the exterior or ideal region, the resistive diffusion and inertia terms can be
71 neglected. We have

$$72 \quad \gamma \psi_{h1} - \psi'_{h0} \gamma \xi = 0 \tag{3}$$

$$73 \quad \left[\frac{1}{r} \frac{d}{dr} \left(r \frac{d\psi_{h1}}{dr} \right) - \frac{m^2}{r^2} \psi_{h1} \right] - \frac{\mu_0 dJ_{z0}}{\psi'_{h0} dr} \psi_{h1} = 0 \tag{4}$$

74 In the interior region, since $\psi''_{h1} \gg \frac{1}{r} \frac{d\psi_{h1}}{dr} \gg \frac{m^2}{r^2} \psi_{h1}$, it yields

$$75 \quad \psi_{h1} - F' x \xi = \frac{r_s^2}{\gamma \tau_R} \psi''_{h1} \tag{5}$$

$$76 \quad \frac{\gamma^2 \tau_A^2}{m^2} \xi'' = -F' x \psi''_{h1} \tag{6}$$

77 where $F' = -q'_s / q_s$, $x = r - r_s$, $\tau_A = r_s \sqrt{\mu_0 \rho} / B_{\theta 0}(r_s)$ and $\tau_R = \mu_0 r_s^2 / \eta$.

78 Through the matching condition of the interior and exterior solutions, we obtain the linear growth
79 rate

$$80 \quad \gamma = \left(\frac{\Gamma(1/4)}{\pi \Gamma(3/4)} \Delta \right)^{4/5} \left(\frac{\eta}{\mu_0} \right)^{3/5} \left(\frac{m q'_s B_{\theta 0}(r_s)}{r_s q_s \sqrt{\mu_0 \rho}} \right)^{2/5}. \tag{7}$$

81 With inclusion of the Hall contribution in the Om's law, the linearized equations for tearing
82 mode instability is modified to be

$$83 \quad \gamma \psi_{h1} - \psi'_{h0} (\gamma + i\omega) \xi = \frac{\eta}{\mu_0} \left[\frac{1}{r} \frac{d}{dr} \left(r \frac{d\psi_{h1}}{dr} \right) - \left(\frac{m^2}{r^2} + \frac{n^2}{R^2} \right) \psi_{h1} \right] + \frac{im}{ner} J_{0\perp} \psi_{h1}, \tag{8}$$

$$\begin{aligned}
& \gamma (\gamma + i\omega) \rho \frac{1}{m} \left[\frac{1}{r} \frac{d}{dr} \left(r \frac{d(r\xi)}{dr} \right) - \frac{m^2}{r^2} (r\xi) \right] \\
84 \quad & = -\frac{m}{\mu_0 r} \psi'_{h0} \left[\frac{1}{r} \frac{d}{dr} \left(r \frac{d\psi_{h1}}{dr} \right) - \frac{m^2}{r^2} \psi_{h1} \right] + \frac{m}{r} \psi_{h1} \frac{dJ_{z0}}{dr}.
\end{aligned} \tag{9}$$

85 The last term in Eq. (8) is associated with the Hall effects. In the exterior or ideal region, Eq. (8)

86 and (9) becomes

$$87 \quad \gamma\psi_{h1} - \psi'_{h0}(\gamma + i\omega)\xi = \frac{im}{ner} J_{0\perp}\psi_{h1}, \quad (10)$$

$$88 \quad \left[\frac{1}{r} \frac{d}{dr} \left(r \frac{d\psi_{h1}}{dr} \right) - \frac{m^2}{r^2} \psi_{h1} \right] - \frac{\mu_0 dJ_{z0}}{\psi'_{h0} dr} \psi_{h1} = 0, \quad (11)$$

89 respectively. From the real and imaginary parts of Eq. (10), it yields

$$90 \quad \gamma\psi_{h1} - \psi'_{h0}\gamma\xi = 0, \quad (12)$$

$$91 \quad -\psi'_{h0}\omega\xi = \frac{m}{ner} J_{0\perp}\psi_{h1}. \quad (13)$$

92 From Eq. (12) and (13), it easily gets

$$93 \quad \omega = -\frac{m}{ner} J_{0\perp} = -\frac{m}{nerB_{h0}} \frac{dp}{dr} = m\omega_*, \quad (14)$$

94 where $\omega_* = -\frac{1}{neBr} \frac{dp}{dr}$ is the diamagnetic rotation frequency. It is suggested that the mode

95 structure in the ideal region is rotated with the diamagnetic frequency due to inclusion of Hall
96 effects.

97 For the case $\omega_* \ll \gamma$, Eq. (5) and (6) for the interior region remain unchanged. Thus, we have
98 the same linear growth rate as in resistive MHD, which means that the diamagnetic rotation of the
99 mode structure in the outer region for Hall MHD will not affect the mode growth rate if $\omega_* \ll \gamma$.

100

101 III. HALL-MHD EQUATIONS IN CLT

102 The full set of the Hall-MHD equations is given as follows:

$$103 \quad \frac{\partial \rho}{\partial t} = -\nabla \cdot (\rho \mathbf{v}) + \nabla \cdot [D\nabla(\rho - \rho_0)] \quad (16)$$

$$104 \quad \frac{\partial p}{\partial t} = -\mathbf{v} \cdot \nabla p - \Gamma p \nabla \cdot \mathbf{v} + \nabla \cdot [\boldsymbol{\kappa} \nabla (p - p_0)] \quad (17)$$

$$105 \quad \frac{\partial \mathbf{v}}{\partial t} = -\mathbf{v} \cdot \nabla \mathbf{v} + (\mathbf{J} \times \mathbf{B} - \nabla p) / \rho + \nabla \cdot [\nu \nabla (\mathbf{v} - \mathbf{v}_0)] \quad (18)$$

$$106 \quad \frac{\partial \mathbf{B}}{\partial t} = -\nabla \times \mathbf{E} \quad (19)$$

107
$$\mathbf{E} = -\mathbf{v} \times \mathbf{B} + \eta(\mathbf{J} - \mathbf{J}_0) + \frac{d_i}{\rho}(\mathbf{J} \times \mathbf{B} - \nabla P_e) \quad (20)$$

108
$$\mathbf{J} = \nabla \times \mathbf{B} \quad (21)$$

109 Where ρ , p , \mathbf{v} , \mathbf{B} , \mathbf{E} , and \mathbf{J} denote the plasma density, the thermal pressure, the plasma velocity,
110 the magnetic field, the electric field, and the current density, respectively. $d_i = c / \omega_{pi}$ is the ion

111 skin length. The subscript “0” denotes the equilibrium quantities. $\Gamma (= 5/3)$ is the ratio of

112 specific heat of plasma. p_e is the electron pressure. The variables are normalized as follows:

113 $\mathbf{B} / B_0 \rightarrow \mathbf{B}$, $\mathbf{x} / a \rightarrow \mathbf{x}$, $\rho / \rho_0 \rightarrow \rho$, $\mathbf{v} / v_A \rightarrow \mathbf{v}$, $t / t_A \rightarrow t$, $p / (B_0^2 / \mu_0) \rightarrow p$,

114 $\mathbf{J} / (B_0 / \mu_0 a) \rightarrow \mathbf{J}$, $\mathbf{E} / (v_A B_0) \rightarrow \mathbf{E}$, $d_i / a \rightarrow d_i$ and $\eta / (\mu_0 a^2 / t_A) \rightarrow \eta$, where a is the

115 minor radius, $v_A = B / \sqrt{\mu_0 \rho}$ is the Alfvén speed, and $t_A = a / v_A$ is the Alfvén time. B_0 and

116 ρ_0 are the magnetic field and the plasma density at the magnetic axis, respectively. For the

117 typical parameters in Tokamak, $n \sim 10^{20}$, $a \sim 1$, $\omega_{pi} \sim 10^{10}$ and $c = 3 \times 10^8$ so $d_i \sim 0.03$.

118 In the previous literatures^{16, 17}, the diamagnetic flow as an initial background flow is added into

119 the momentum equation to study diamagnetic rotation effects on the tearing mode instability, i.e.,

120
$$\frac{\partial \mathbf{v}}{\partial t} = -\mathbf{v} \cdot \nabla \mathbf{v} - \mathbf{v}_* \cdot \nabla \mathbf{v} + (\mathbf{J} \times \mathbf{B} - \nabla p) / \rho \quad (22)$$

121 In this equation the contribution of $\mathbf{v} \cdot \nabla \mathbf{v}_*$ is neglected. However, these terms are not guaranteed

122 to be zero. In our simulations, the diamagnetic rotation effects on the tearing mode instability are

123 investigated self-consistently by using the Hall-MHD equations.

124

125 IV. SIMULATION RESULTS

126 A. m/n=2/1 tearing mode

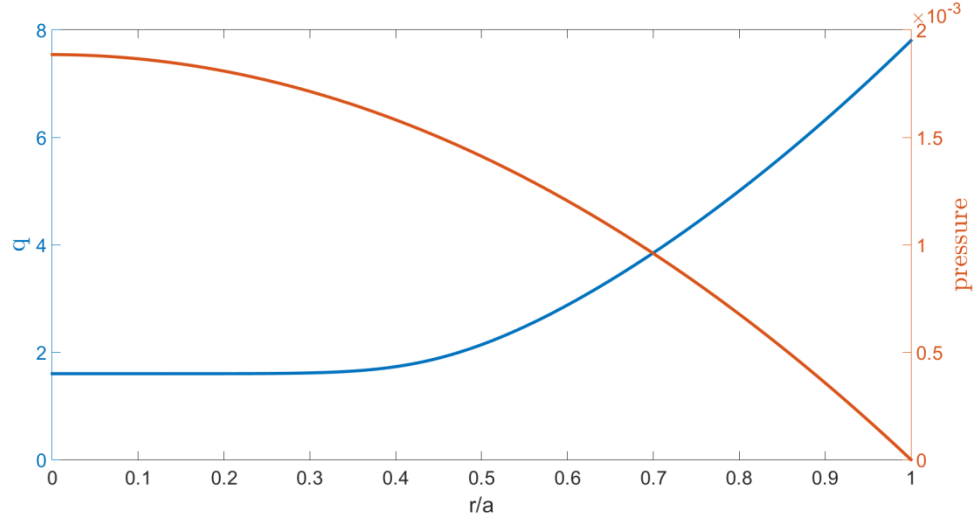
127 The parameters with a toroidal tokamak configuration are chosen as follows: the major radius

128 $R_0 = 4$ and the minor radius $a = 1$. The initial equilibrium profiles of the safety factor q and the

129 plasma pressure p are shown in Figure 1. The equilibrium magnetic field B_0 and the current

130 density J_0 are obtained from the NOVA²² code. Other diffusion parameters used in our

131 simulations are the resistivity $\eta = 1 \times 10^{-5}$, the viscosity $\nu = 1 \times 10^{-6}$, the plasma diffusivity
 132 $D = 1 \times 10^{-6}$, and the conductivity $\kappa = 5 \times 10^{-5}$. The larger conductivity is used to suppress
 133 ballooning modes. With the given profile, the most unstable tearing mode is the m/n=2/1 mode
 134 occurs at the $q=2$ rational surface.

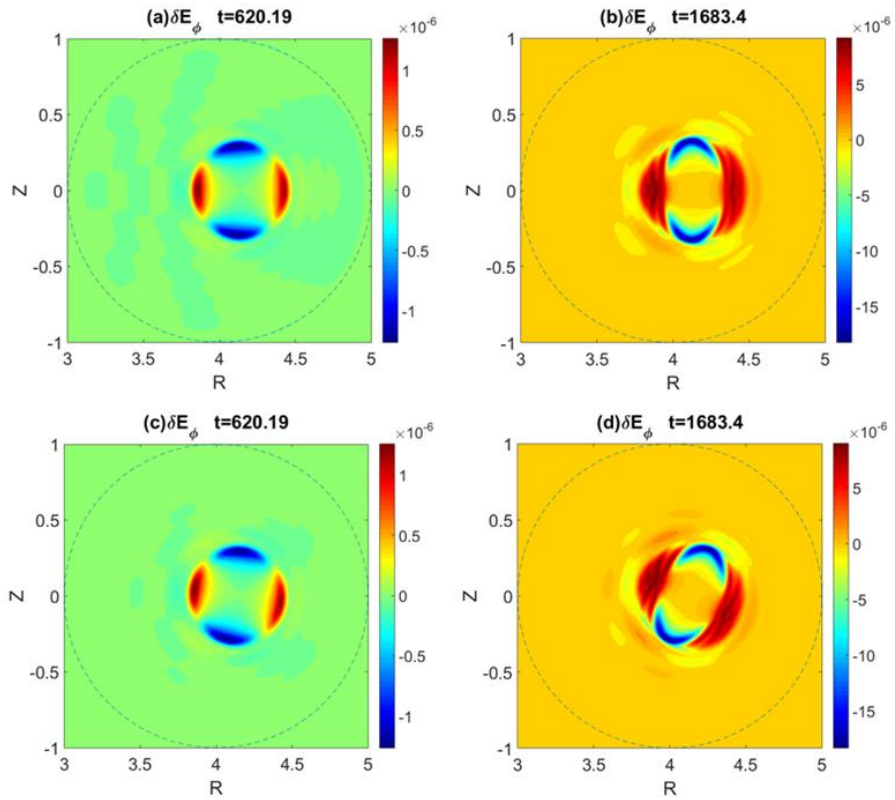


135 Figure 1 .Initial profiles of the safety factor q and the plasma pressure p .

137

138 Figure 2 gives the mode structures (δE_ϕ) in the $\phi = 0$ cross-section at (a), (c) $t=620$
 139 t_A and (b), (d) $t=1683 t_A$ for cases with/without Hall effects. It is clearly indicated that there is a
 140 slow rotation of the mode structure for Hall-MHD. The mode structure at $t=1683 t_A$ has been
 141 rotated about 30 degree, which gives the period to be about $T_s \sim 2 \times 10^4 t_A$. After inserting the
 142 parameters used in the simulation into Equation (14), we have $T_r \sim 1.7 \times 10^4 t_A$ which is in a
 143 good agreement with that from the simulation. From the pressure profile, the pressure inside the
 144 $q=2$ resonant surface becomes gradually flattening. The low pressure gradient leads to a slower
 145 rotation speed. The mode structure will slow down overall mode rotation due to the dragging
 146 effect of the slower rotation of the core region. This is why the rotation period in the simulation
 147 is slightly longer than that from the theoretical calculation.

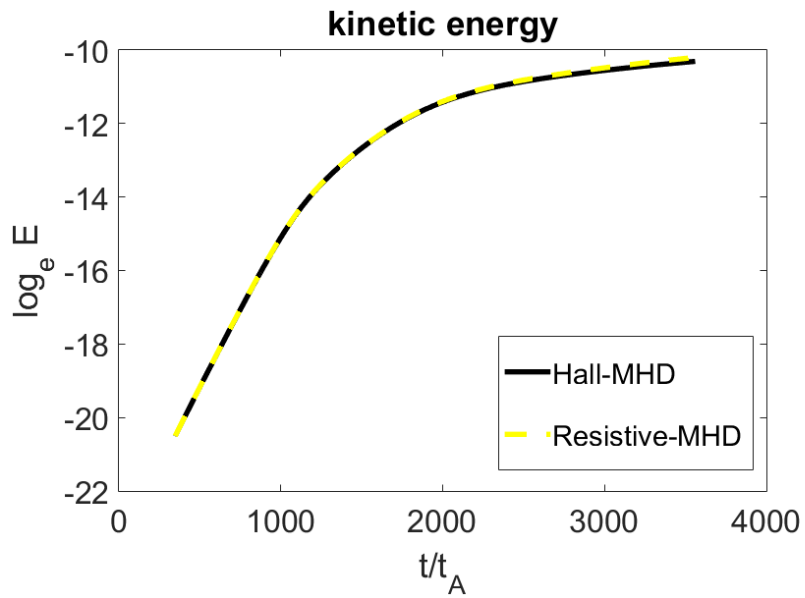
148



149

150 Figure 2 .The mode structure (δE_ϕ) from resistive MHD and Hall MHD at $t=620 t_A$ and $t=1683 t_A$.

151



152

153 Figure 3 .The time evolution of the kinetic energy with/without Hall effects for the $m/n=2/1$ tearing
154 mode.

155

156 The time evolution of the kinetic energy with/without Hall effects for the $m/n=2/1$

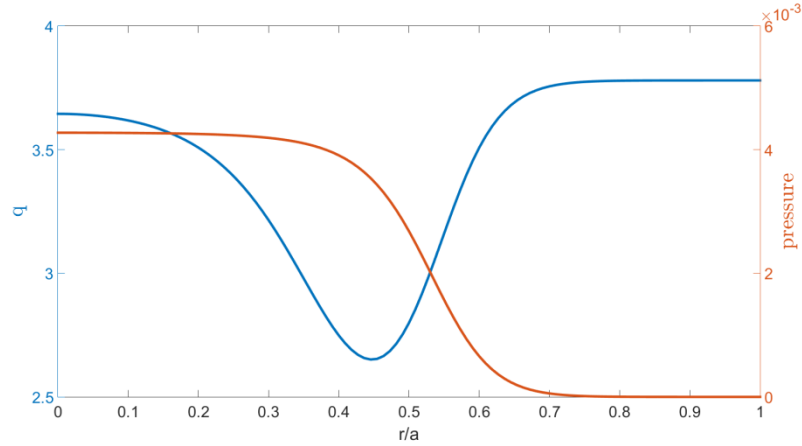
157 tearing mode is given in Figure 3. It is found that the linear growth rate is $\gamma = 0.0084$ that is
158 much larger than the rotation frequency of the mode structure in Hall MHD. As we expected,
159 there are the same linear growth rates of the $m/n=2/1$ mode for cases with/without Hall effects
160 because the current sheet thickness is still larger than the ion inertial length in the linear phase. In
161 the nonlinear phase, the reconnection rate in the slab geometry will largely increase in Hall MHD.
162 In the present simulation with Tokamak geometry, reconnection rates are no change with/without
163 Hall effects, which may be associated with the diamagnetic rotation of the mode structure in Hall
164 MHD. The mode rotation can prevent the current sheet thinning.

165

166 **B. Double tearing mode**

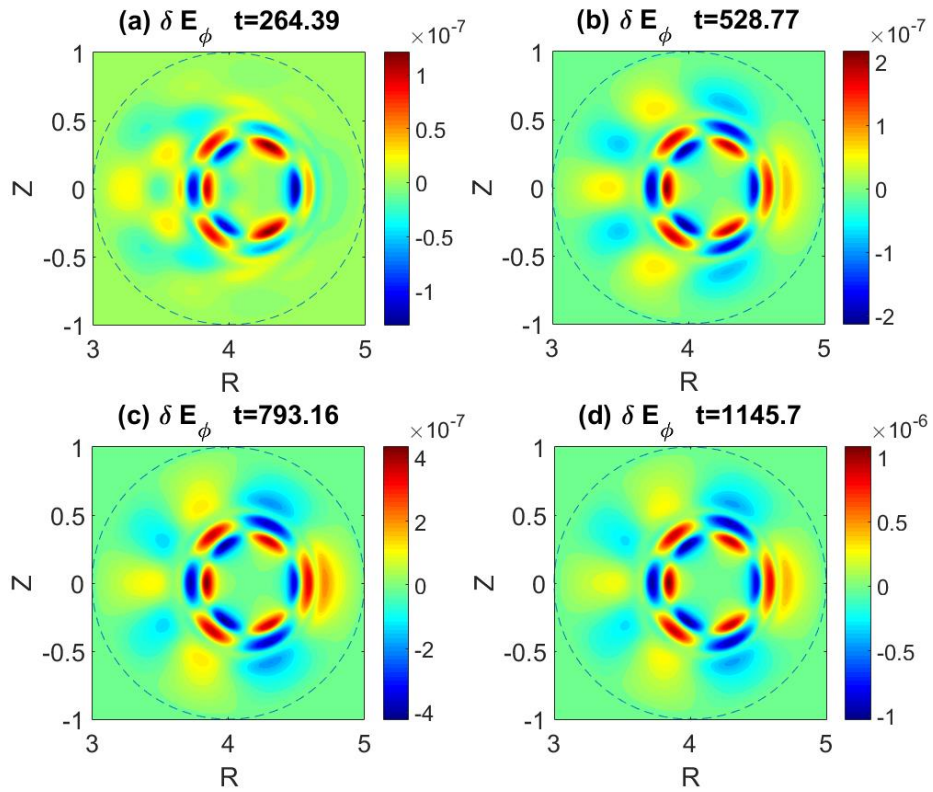
167 Previous studies²³ suggests that for a reserved q profile, tearing mode instabilities in two
168 resonant surfaces will excite each other and grow much faster than a single tearing mode because
169 the growing mode in one resonant surface becomes an external driven source that accelerates the
170 mode development in another resonant surface.

171 In the previous subsection for the single tearing mode, it has been shown that the mode
172 structure rotates at the diamagnetic frequency due to inclusion of Hall effects and the rotation
173 speed of the mode structure depends on the local pressure gradient. It can be expected that
174 different rotation frequencies of mode structures, due to different pressure gradients, will largely
175 affect the dynamic evolution of a double tearing mode. We artificially construct an equilibrium
176 with reverse-sheared q profile and different gradients of the plasma pressure to study double
177 tearing mode instability. The initial q and pressure profiles are showed in Figure 4. With the
178 range of q from 2.6 to 3.8, the most unstable modes should be the $m/n=3/1$ mode which takes
179 place at the two resonant surfaces with $q=3$.



180
181
182

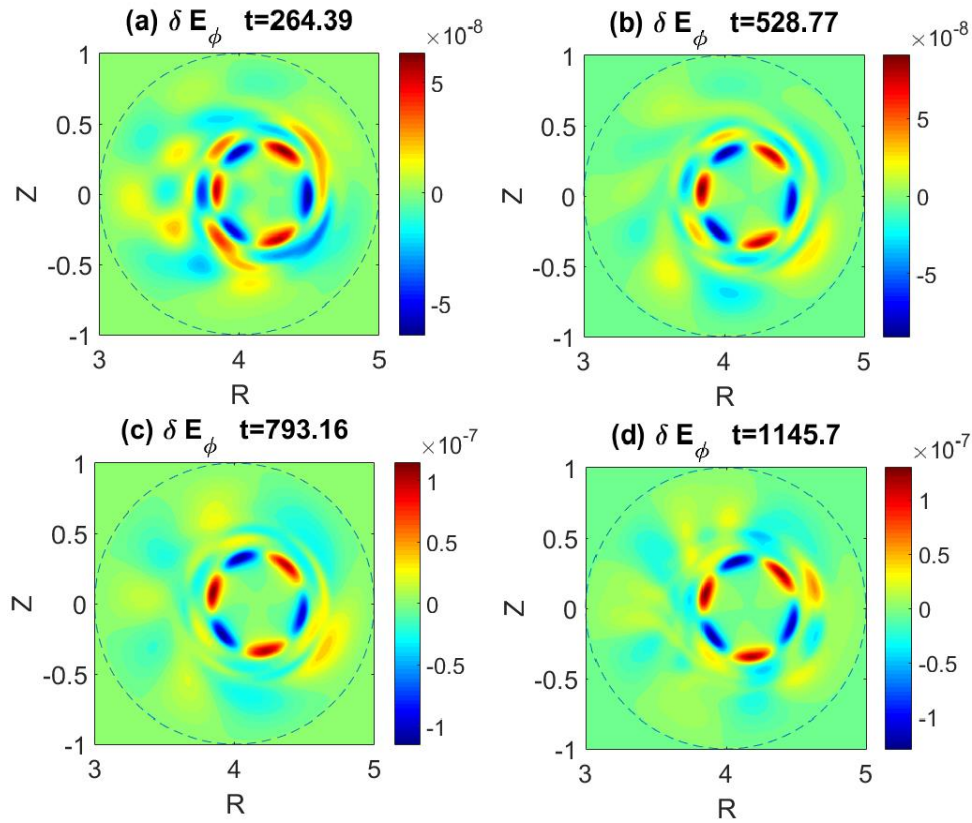
Figure 4. The initial q and pressure profile for $m/n=3/1$ double tearing mode instability.



183
184

Figure 5. The snapshots of mode structures (δE_ϕ) from resistive-MHD.

185 The snapshots of mode structures (δE_ϕ) from resistive MHD are shown in Figure 5. It
186 is evident that the perturbations at the two resonant surfaces have opposite polarities and this
187 property of the opposite polarities remains in the whole simulation period. The opposite
188 polarities of the mode perturbations becomes mutual driven sources that accelerate the
189 development of double tearing mode instability persistently. Therefore, the growth rate of the
190 double tearing mode is much faster than that of a single tearing mode in resistive MHD.



192

193

Figure 6. The snapshots of the mode structures (δE_ϕ) from Hall MHD.

194

195

196

197

198

199

200

201

202

203

204

205

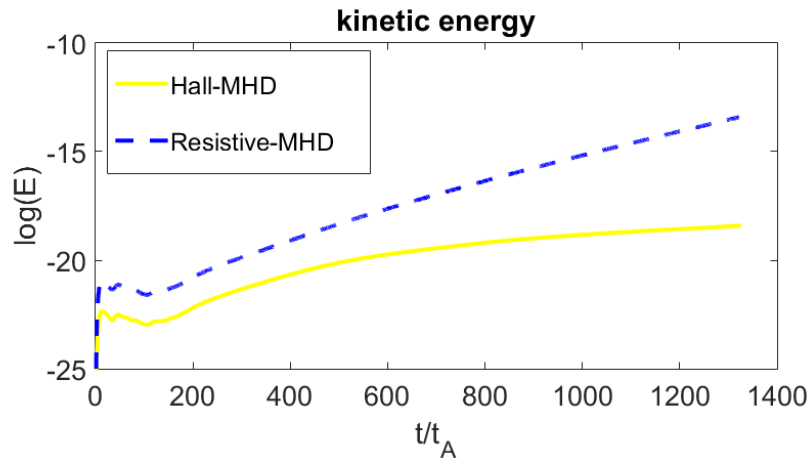
206

207

With inclusion of Hall effect, the simulation and theoretical results of the single tearing mode suggests that the mode structure at the outer resonant surface rotates with the frequency $\omega = 3\omega_*$ while the mode structure at the inner resonant surface is stationary due to the flatten pressure profile, which is quite evident from simulation results as given in Figure 6. In the simulation, the mode structure in the outer resonant surface rotates clockwise while the inner mode structure almost remains at rest. The perturbations of two tearing modes gradually switch from anti-phase to in-phase. In other words, the perturbations for the two modes gradually evolve from mutual acceleration to mutual suppression, which is clearly indicated in Figure 6 that the growth rates of the amplitudes of the mode structure reduces with time and the mode finally saturates.

The time evolutions of the kinetic energy for double tearing modes from resistive-MHD and Hall MHD are shown in Figure 7. It is clearly indicated that the growth rate of the double tearing mode in resistive MHD is much larger than in Hall MHD. The kinetic energy in resistive MHD continuously increases and there is no saturation observed in the simulation period. But the

208 kinetic energy in Hall MHD has a low growth rate and quickly saturates at a very low level.



209

210 Figure 7. The time evolution of the kinetic energy for double tearing modes from resistive-MHD and
211 Hall MHD.

212 V. SUMMARY AND DISCUSSION

213 In magnetic confined fusion device such as Tokamak, the thermal plasma pressure decreases
214 away from the central core region. The pressure gradient leads to a diamagnetic rotation of plasma.
215 The diamagnetic rotations resulted from ion or electron pressure usually play different role on
216 plasma dynamics due to the large mass ratio. The diamagnetic rotation associated with ion
217 pressure causes a plasma flow while it related to the electron pressure leads to the rotation of the
218 magnetic field perturbation due to the frozen-in condition. In Hall MHD, the pressure is only from
219 the electrons because the cold ions are assumed. Thus, we should only observe the diamagnetic
220 rotation of the mode structure without the plasma rotation flow.

221 Tearing mode instability is one of the most important dynamic processes in space and
222 laboratory plasmas. It is suggested that Hall effects in the slab geometry could cause the fast
223 development and perturbation structure rotation of the tearing mode and become non-negligible.
224 In this paper, we use the new developed high accuracy nonlinear MHD code (CLT) to study Hall
225 effects on the dynamic evolution of tearing modes with Tokamak geometries. It is found that the
226 rotation speed of the mode structure from the simulation is in a good agreement with that from the
227 analytical theory in a single tearing mode. The phenomenon of fast growth of tearing mode
228 instability is not observed, which may be associated with the rotation of the reconnection region.

229 The Hall effects on dynamic evolution of double tearing mode is also conducted out.
230 With an artificial constructed pressure to amplify the different diamagnetic rotation speeds at two

231 resonant surfaces, it is found that the perturbations of two tearing modes in Hall MHD gradually
232 switch from anti-phase to in-phase while the perturbations in resistive MHD is persistently
233 anti-phase. In Hall MHD, the mutual driven perturbations with opposite polarities gradually
234 evolve to the mutual suppressed perturbations with the same polarities which cause the lower
235 growth rate of the double tearing mode and the mode amplitude saturates at a very low level.

236

237 ACKNOWLEDGEMENTS

238 We would like to thank Jia Zhu, Lingjie Li and Zhichen Feng for their helpful comments.
239 This work is supported National Magnetic Confinement Fusion Science Program of China under
240 Grant No. 2013GB104004 and 2013GB111004, the Special Project on High-performance
241 Computing under the National Key R&D Program No. 2016YFB0200603, Fundamental Research
242 Fund for Chinese Central Universities, the National Natural Science Foundation of China under
243 Grant No. 41474123.

244

245 References

- 246 1. B. U. Ö. Sonnerup, P. J. Baum, J. Birn, S. W. H. Cowley, T. G. Forbes, A. B. Hassam, S. W. Kahler, W.
247 H. Matthaeus, W. Park and G. Paschmann, *Reconnection of magnetic fields*. (Cambridge University
248 Press, 2007).
- 249 2. S. Tsuneta, *Astrophysical Journal* **456** (456), 840 (1996).
- 250 3. E. J. Strait, L. Lao, A. G. Kellman, T. H. Osborne, R. Snider, R. D. Stambaugh and T. S. Taylor,
251 *Physical Review Letters* **62** (11), 1282-1285 (1989).
- 252 4. R. J. La Haye, L. L. Lao, E. J. Strait and T. S. Taylor, *Nuclear Fusion* **37** (37), 397-401 (1997).
- 253 5. R. B. White, *Review of Modern Physics* **58** (1), 183-207 (1986).
- 254 6. D. Biskamp, *Magnetic reconnection in plasmas*. (Cambridge University Press, 2005).
- 255 7. R. M. Kulsrud, *Plasma physics for astrophysics*. (Princeton University Press, 2005).
- 256 8. J. A. Wesson, R. D. Gill, M. Hugon, F. C. Schüller, J. A. Snipes, D. J. Ward, D. V. Bartlett, D. J.
257 Campbell, P. A. Duperrex and A. W. Edwards, *Nuclear Fusion* **29** (4), 641-666 (1989).
- 258 9. F. C. Schuller, *Plasma Physics & Controlled Fusion* **37** (11), A135-A162(128) (1995).
- 259 10. M. Shimada, D. J. Campbell, V. Mukhovatov, M. Fujiwara, N. Kirneva, K. Lackner, M. Nagami, V. D.
260 Pustovitov, N. Uckan and J. Wesley, *MMW - Fortschritte der Medizin* **157** (21-22), 44-44 (2007).
- 261 11. H. P. Furth, J. Killeen and M. N. Rosenbluth, *Physics of Fluids (1958-1988)* **6** (2), 130-134 (1963).
- 262 12. L. M. Malyskin, *Physical Review Letters* **101** (22), 4473-4475 (2008).
- 263 13. X. Wang, A. Bhattacharjee and Z. W. Ma, *Journal of Geophysical Research Atmospheres* **105** (A12),
264 27633-27648 (2000).
- 265 14. Z. W. Ma and A. Bhattacharjee, *Journal of Geophysical Research Space Physics* **106** (A3),
266 3773-3782 (2001).
- 267 15. G. Ara, B. Basu, B. Coppi, G. Laval, M. N. Rosenbluth and B. V. Waddell, *Annals of Physics* **112** (2),

- 268 443-476 (1978).
- 269 16. Q. Yu, S. Günter, S. Günter, K. Lackner and K. Lackner, *Nuclear Fusion* **55** (11) (2015).
- 270 17. F. D. Halpern, H. Lütjens and J. F. Luciani, *Physics of Plasmas* **18** (18), 102501-102501-102509
271 (2011).
- 272 18. Z. Chang, W. Park, E. D. Fredrickson, S. H. Batha, M. G. Bell, R. Bell, R. V. Budny, C. E. Bush, A.
273 Janos and F. M. Levinton, *Physical Review Letters* **77** (17), 3553-3556 (1996).
- 274 19. A. Bierwage, S. Hamaguchi, M. Wakatani, S. Benkadda and X. Leoncini, *Physical Review Letters* **94**
275 (6), 065001 (2004).
- 276 20. S. Wang and Z. W. Ma, *Physics of Plasmas* **22** (12), 122504 (2015).
- 277 21. S. Wang, Z. W. Ma and W. Zhang, *Physics of Plasmas* **23** (5), 052503 (2016).
- 278 22. C. Z. Cheng and M. S. Chance, *Journal of Computational Physics* **71** (1), 124-146 (1986).
- 279 23. C. L. Zhang and Z. W. Ma, *Physics of Plasmas* **18** (18), 052307 (2011).
- 280